Shock and Vibration 10 (2003) 187–194
IOS Press

Dynamic stability of rotating blades with transverse cracks

T.Y. Ng[a,b,*], K.Y. Lam[a] and Hua Li[a]
[a]*Institute of High Performance Computing, 1 Science Park Road, #01-01 The Capricorn Singapore Science Park II, Singapore 117528*
[b]*School of Mechanical and Production Engineering, Nanyang Technological University 50 Nanyang Avenue, Singapore 639798*

Received 4 October 2001
Revised 12 December 2002

Abstract. In this paper, the main objective is to examine the effects of transverse cracks on the dynamic instability regions of an axially loaded rotating blade. The blade is modeled as an Euler-Bernoulli beam. To reduce the governing equations to a set of ordinary differential equations in matrix form, Hamilton's principle is used in conjunction with the assumed-mode method. The crack is accounted for by considering the energy release rate and the parametric instability regions are obtained using Bolotin's first approximation. Benchmark results are presented for cracked rotating blades at different rotating speeds, crack lengths and crack positions.

Keywords: Rotating blade, transverse crack, dynamic stability, parametric resonance, Hamilton's principle, assumed-mode method, Bolotin's first approximation

1. Introduction

The dynamic behaviour of a beam may change due to the presence of cracks. The changes in the dynamic characteristics due to the changes in the crack lengths are important with respect to the science of crack detection and design of structures. Adams et al. [1] showed that for the axial vibration of a uniform bar, the reduction in stiffness of the bar due to the presence of a crack could be modelled by the introduction of a linear spring. However, the relationship between the magnitude of the spring constant and the crack length was not determined. Ju et al. [2] theoretically related the magnitude of the equivalent linear spring constant to the length of the crack in the beam based on fracture mechanics. Several researchers, Moshrefi et al. [3], Ju and Mimovich [4] and Rizos et al. [5], have experimentally diagnosed the changes in natural frequency due to existing cracks and have concluded the feasibility of modelling a crack by an appropriate combination of linear and torsional springs.

Using perturbation and transfer matrix methods, the changes in the natural frequencies due to the presence of cracks were computed by Gudmundson [6,7]. Papadopoulos and Dimarogonas [8] modelled a crack using a 2×2 compliance matrix to describe the local flexibility in the analysis of the coupled longitudinal and bending vibrations of a cracked shaft. In analysing the coupled vibration of a cracked rotor, Papadopoulos and Dimarogonas [9] represented the local flexibility by a 6×6 compliance matrix. A finite element method for the analysis of cracked beams was developed by Haisty and Springer [10] and the crack in this case was modelled as a linear spring for axial vibrations and a torsional spring for flexural vibrations. Qian et al. [11] also presented an element stiffness matrix for a cracked beam based on the principles of fracture mechanics. The Rayleigh quotient was used by Chondros and Dimarogonas [12] for estimating the change in the nat-

*Corresponding author. E-mail: mtyng@ntu.edu.sg.

ISSN 1070-9622/03/$8.00

ural frequencies and modes for the torsional vibration of a cracked rotor and also for the in-plane vibration of frames. The small change in the local stiffness at the crack was introduced into the Rayleigh quotient from which the variation in the eigenvalue was computed. Shen and Pierre [13], using both an approximate Galerkin formulation and finite element method obtained the natural frequencies and modes for the transverse vibrations of simply supported Bernoulli-Euler beams with a pair of symmetric double-sided cracks at the mid-span position. Dimarogonas and Paipetis [14] constructed a crack related 5×5 local flexibility matrix for a rectangular beam from principles of fracture mechanics and analyzed the coupling effects between the axial loading and lateral bending. Subsequently, Dimarogonas and Papadopoulos [15] expanded the work to a circular shaft with a transverse crack and calculated the flexibility coefficients due to bending in two perpendicular directions.

Examples of radially rotating beams and blades include rotor blades, propellers, turbines, robotic arms and numerous other parts that are commonly found in rotating machineries. This field has been studied in the last few decades in relation to the behaviour of rotating blades in turbomachineries. As such, an extensive literature on radially rotating uniform, pretwisted and tapered beams are readily available. Prior documented works include Sutherland [16], Renard and Rabowski [17], Likins et al. [18], Anderson [19], Swaminathan and Rao [20], Hodges and Ruthoski [21] and Subrahnanvam et al. [22]. These studies compose both uniform and pretwisted beams rotating at constant angular velocities. Other studies of similar configurations include Kane et al. [23] who modeled a Timoshenko beam built into a rigid base and undergoing general three-dimensional motions. Rotating beams subjected to base excitations have commonly been used to model propellers, helicopter rotor blades and mobile linkages of robots. Hammond [24] treated a non-isotropic hub and four-bladed rotor with the incorporation of the base movements.

In the present study, the effects of transverse cracks on the parametric resonance of an axially loaded rotating blade modeled as an Euler-Bernoulli beam is investigated. Hamilton's energy principle is used in conjunction with the assumed-mode method to obtain a set of ordinary differential equations in matrix form the stability of which is analyzed using Bolotin's [25] first approximation. The crack is accounted for by considering the energy release rate. The analysis is carried out for various rotating speeds, crack lengths and crack positions.

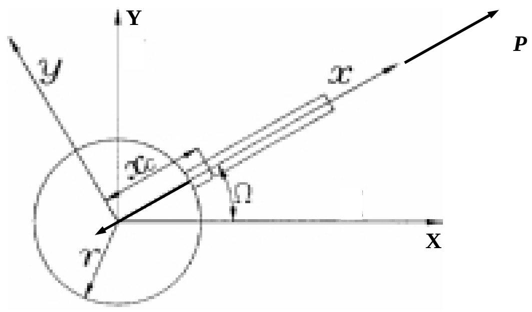

Fig. 1. Coordinate system of the rotating blade.

2. Theory and formulation

Consider a uniform slender beam system as shown in Fig. 1 with one end clamped to a rotating hub of radius r and rotating with constant angular velocity Ω. An axial harmonic loading in the longitudinal direction of the beam is considered

$$P = P_o + P_s \cos \omega t \tag{1}$$

where P_o is the stationary component and P_s is the amplitude of the harmonic component of the loading. The beam is considered as an Euler-Bernoulli beam of constant cross-sectional area and thus only the transverse deflection v is considered. The potential energy arising from the above loading is

$$U_p = P \int_r^{r+L} (v_{,x})^2 dx \tag{2}$$

where the subscripts after the commas indicate the partial differentiation with respect to, and the kinetic energy of the beam is given as

$$T = \frac{\rho A}{2} \int_r^{r+L} \{(v_{,t})^2 + 2x\Omega v_{,t} + (x^2 + v^2)\Omega^2\} dx \tag{3}$$

where ρ denotes the mass density, E the elastic modulus, A the cross-sectional area, I the area moment of inertia, and L the length. The potential energy due to bending is

$$U_v = \frac{EI}{2} \int_r^{r+L} (v_{,xx})^2 dx \tag{4}$$

and that due to the initial stress is

$$U_\Omega = \frac{\rho A}{4} \Omega^2 \int_r^{r+L} ((r+L)^2 - x^2)(v_{,x})^2 dx \tag{5}$$

From Dimarogonas and Paipetis [15], the energy release of the crack is

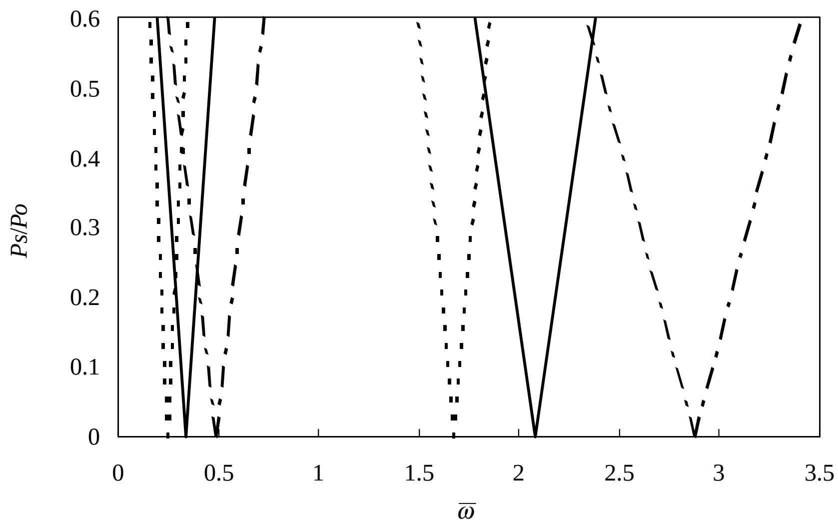

Fig. 2. First two instability regions for a rotating beam with a single crack at mid-span, $\overline{\Omega} = 1$ and $a/h = 0.5$. '-.-.-' $L = 0.8$ m, '–' $L = 1.0$m, '- - -' $L = 1.2$ m.

$$U_c = b\int_0^a J(a)da \tag{6}$$

where b is the width of the beam and

$$J(a) = \frac{K_c^2(1-\nu^2)}{E} \tag{7}$$

where ν is the Poisson's ratio, a is the crack depth and

$$K_c = \frac{6P_c}{bh^2}(\pi a)^{1/2} F_c\left(\frac{a}{h}\right) \tag{8}$$

$$F_c\left(\frac{a}{h}\right) = \frac{0.92 + 0.2(1-\sin(\pi a/2h))^4}{\cos(\pi a/2h)} \times \left(\frac{2h}{\pi a}\tan(\pi a/2h)\right)^{1/2} \tag{9}$$

$$P_c = EI(v,_{xx})^2|_{x=x_c} \tag{10}$$

where h is the beam height. The released energy of the crack can be simplified to the form

$$U_c = 3EIb(1-\nu^2)C_{55} \int_r^{r+L} \delta(x-x_c)(v,_{xx})^2 dx \tag{11}$$

$$C_{55} = \int_0^{a/h} \pi\left(\frac{a}{h}\right) F_c^2\left(\frac{a}{h}\right) d\left(\frac{a}{h}\right) \tag{12}$$

Using the assumed-mode method, see Wu and Huang [26], the beam deformation can be approximated in the following form

$$v(x,t) = \sum_{i=1}^{N} V_i(x) q_i(t) \tag{13}$$

where $q_i(t)$ is a generalized coordinate and $V_i(x)$ is the ith normalized mode of a non-rotating clamped-free beam. The equations of motion in matrix form can then be written in matrix form as

$$[\mathbf{M}]\{\ddot{\mathbf{q}}\} + [[\mathbf{K}] + \cos\omega t[\mathbf{Q}]]\{\mathbf{q}\} = 0 \tag{14}$$

$$M_{ij} = \rho A \int_r^{r+L} V_i(x)V_j(x)dx \tag{15}$$

$$[\mathbf{K}] = [\mathbf{K}^v + \mathbf{K}^\Omega + \mathbf{K}^c + \mathbf{K}^P] \tag{16}$$

$$K_{ij}^v = EI\int_r^{r+L} V_i(x),_{xx} V_j(x),_{xx} dx \tag{17}$$

$$K_{ij}^\Omega = \rho A\Omega^2 \int_r^{r+L} V_i(x) \left\{ \begin{array}{l} xV_j(x),_x - V_j(x) - V_j(x),_{xx} \\ \times\frac{1}{2}((r+L)^2 - x^2) \end{array} \right\} dx \tag{18}$$

$$K_{ij}^c = 6EIb(1-\nu^2)C_{55}V_i(x),_{xx}|_{x=x_c} V_j(x),_{xx}|_{x=x_c} \tag{19}$$

$$K_{ij}^P = P_o\int_r^{r+L} V_i(x),_x V_j(x),_x dx \tag{20}$$

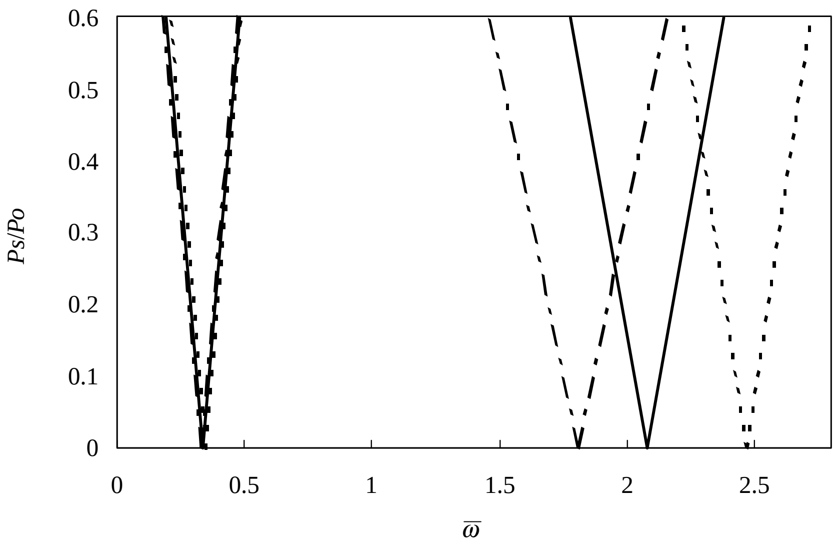

Fig. 3. First two instability regions for a rotating beam with a single crack at mid-span, $L = 1.0$ m and $a/h = 0.5$. '-.-.-' $\overline{\Omega} = 0.5$, '–' $\overline{\Omega} = 1$, '- - -' $\overline{\Omega} = 2$.

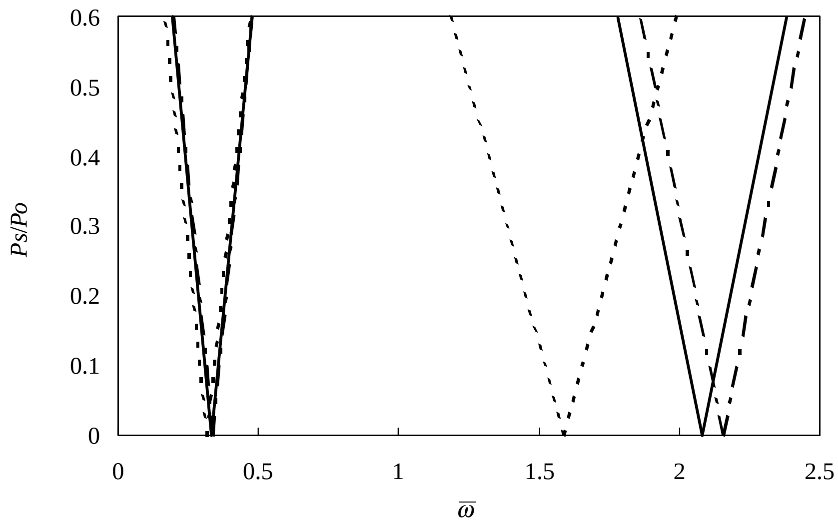

Fig. 4. First two instability regions for a rotating beam with a single crack at mid-span, $\overline{\Omega} = 1$ and $L = 1.0$ m. '-.-.-' $a/h = 0.25$, '– ' $a/h = 0.50$, '- - -' $a/h = 0.75$.

$$Q_{ij} = P_s \int_r^{r+L} V_i(x)_{,x} V_j(x)_{,x} \, dx \tag{21}$$

To obtain the principal instability regions, Bolotin's [25] method is applied to the Mathieu-Hill form of Eq. (14). In this method, we seek the periodic solution with period $2T$ in the form

$$\mathbf{q} = \sum_{k=1,3,5,\ldots}^{\infty} \mathbf{f}_k \sin \frac{k\omega t}{2} + \mathbf{g}_k \cos \frac{k\omega t}{2} \tag{22}$$

For principal instability, Bolotin's [25] first approximation, associated with the 2ω harmonic, is given by the substitution of the following simplified expression

$$\mathbf{q} = \mathbf{f} \sin \frac{\omega t}{2} + \mathbf{g} \cos \frac{\omega t}{2} \tag{23}$$

where $\mathbf{f}$ and $\mathbf{g}$ are arbitrary vectors. It is well known that the secondary instability regions associated with the ω harmonic are significantly smaller than the principal instability regions associated with the 2ω harmonic. In most practical applications, these already

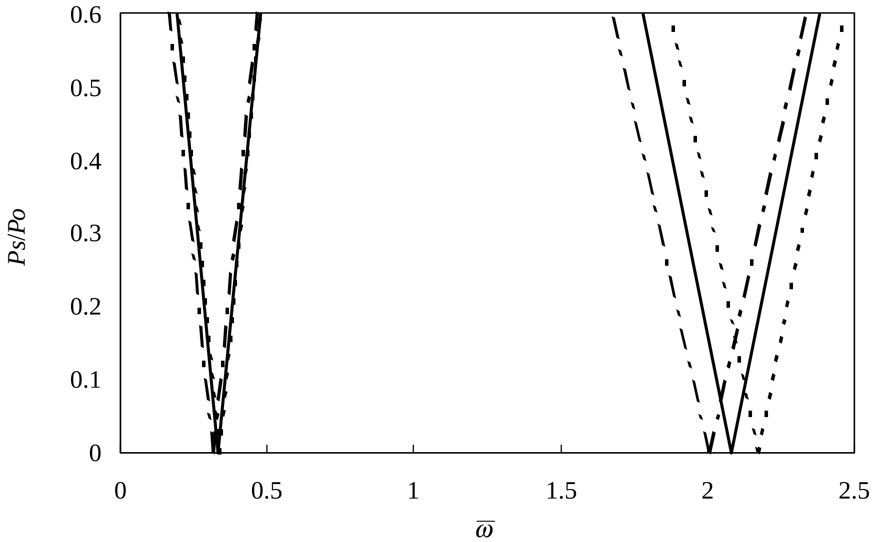

Fig. 5. First two instability regions for a rotating beam with a single crack, $L = 1.0$ m, $\overline{\Omega} = 1$ and $a/h = 0.5$. '-.-.-' $\overline{x}_c = 0.25$, '–' $\overline{x}_c = 0.5$, '- - -' $\overline{x}_c = 0.75$.

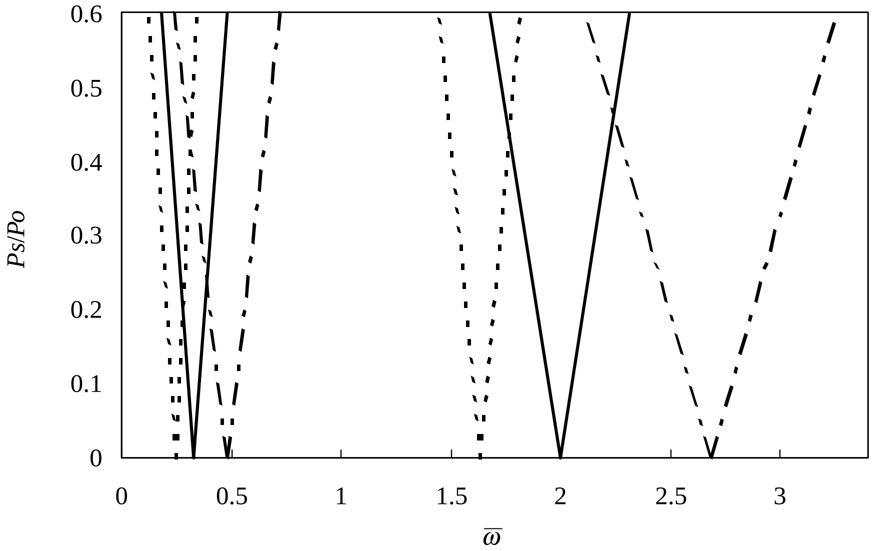

Fig. 6. First two instability regions for a rotating beam with double cracks at $\overline{x}_{cmean} = 0.5L$, $\overline{\Omega} = 1$ and $a/h = 0.5$. '-.-.-' $L = 0.8$ m, '–' $L = 1.0$ m, '- - -' $L = 1.2$ m.

very narrow secondary regions are very often damped away. Substitution into governing equation and equating coefficients of $\sin(\omega t/2)$ and $\cos(\omega t/2)$ terms, we obtain a set of linear homogeneous algebraic equations in terms of $\mathbf{f}$ and $\mathbf{g}$, and for non-trivial solutions

$$\begin{vmatrix} \left(-\frac{1}{4}\omega^2\mathbf{M}_{IJ} + \mathbf{K}_{IJ} - \frac{1}{2}\mathbf{Q}_{IJ}\right) & 0 \\ 0 & \left(-\frac{1}{4}\omega^2\mathbf{M}_{IJ} + \mathbf{K}_{IJ} + \frac{1}{2}\mathbf{Q}_{IJ}\right) \end{vmatrix} = 0 \quad (24)$$

Rearrangement leads to a generalized eigenvalue problem

$$\left| \begin{bmatrix} \mathbf{K}_{IJ} - \frac{1}{2}\mathbf{Q}_{IJ} & 0 \\ 0 & \mathbf{K}_{IJ} + \frac{1}{2}\mathbf{Q}_{IJ} \end{bmatrix} - \omega^2 \begin{bmatrix} \frac{1}{4}\mathbf{M}_{IJ} & 0 \\ 0 & \frac{1}{4}\mathbf{M}_{IJ} \end{bmatrix} \right| = 0 \quad (25)$$

The eigenvalues define the boundaries between the stable and unstable regions.

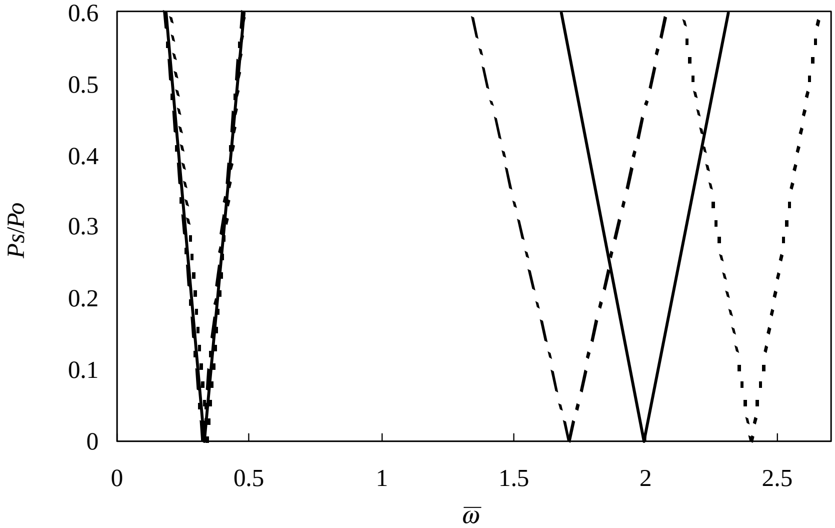

Fig. 7. First two instability regions for a rotating beam with double cracks at $\overline{x}_{cmean} = 0.5L$, $L = 1.0$ m and $a/h = 0.5$. '-.-.-' $\overline{\Omega} = 0.5$, '–' $\overline{\Omega} = 1$, '- - -' $\overline{\Omega} = 2$.

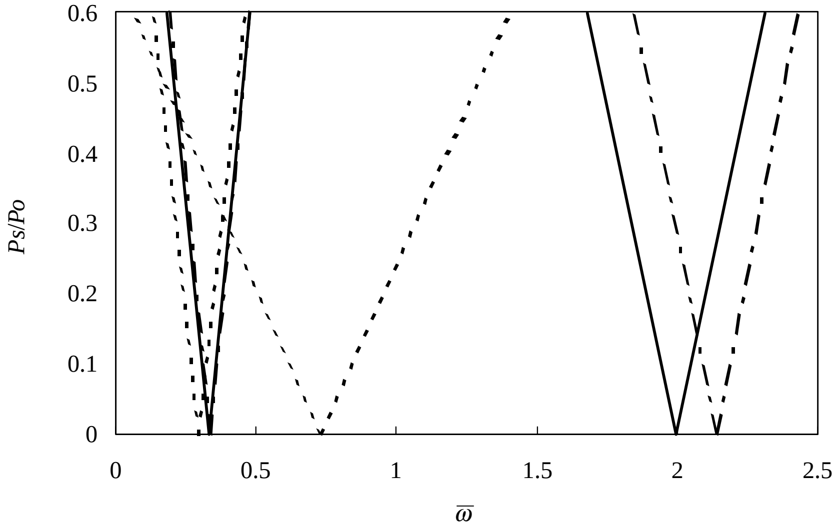

Fig. 8. First two instability regions for a rotating beam with double cracks at $\overline{x}_{cmean} = 0.5L$, $\overline{\Omega} = 1$ and $L = 1.0$ m. '-.-.-' $a/h = 0.25$, '– ' $a/h = 0.50$, '- - -' $a/h = 0.75$.

3. Results and discussions

In the following discussion, the normalized crack position is

$$\overline{x}_c = \frac{x_c - r}{L} \tag{26}$$

and the loading frequency, rotational speed and natural frequency are nondimensionalized as

$$\overline{\omega} = \omega \frac{1}{r^2}\sqrt{\frac{EI}{\rho A}} \tag{27}$$

$$\overline{\Omega} = \Omega \frac{1}{L^2}\sqrt{\frac{EI}{\rho A}} \tag{28}$$

$$\overline{\omega}_n = \omega_n \frac{1}{L^2}\sqrt{\frac{EI}{\rho A}} \tag{29}$$

Dynamic stability results for a rotating beam with a single crack are presented in Figs 2 to 5. These figures show the unstable regions for the first two modes as various parameters are varied. Each set of lines

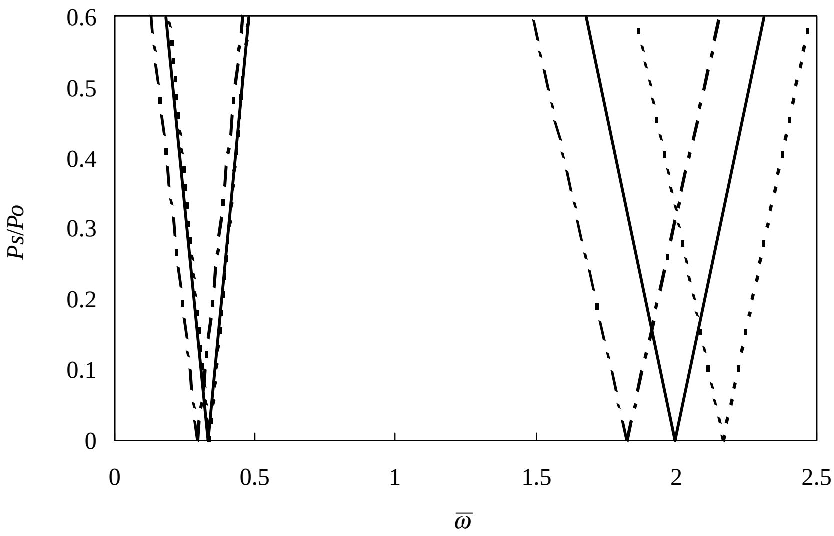

Fig. 9. First two instability regions for a rotating beam with double cracks, $L = 1.0$ m, $\overline{\Omega} = 1$ and $a/h = 0.5$. '-.-.-' $\overline{x}_{cmean} = 0.25$, '–' $\overline{x}_{cmean} = 0.5$, '- - -' $\overline{x}_{cmean} = 0.75$.

originating from the abscissa represents the boundary between the stable and unstable regions. The region between each set of lines constitutes the unstable region while that outside the lines constitutes the stable region. The loading is overall tensile with $\overline{P}_o = 1$ where

$$\overline{P}_o = \frac{P_o L^2}{EI} \tag{30}$$

and the cross section of the beam is taken to be square with the length to beam height ratio being $L/h = 50$ with hub radius $r = 0.2$ m and length $L = 1$ m unless otherwise stated.

In Fig. 2, the length of the beam is varied, hub radius being kept constant. It is observed that modest changes in the length can cause substantial changes in the position as well as size of the unstable regions with the changes more pronounced in the second mode. Shorter length beams are observed to have unstable regions at higher values on the excitation frequency axis. This is intuitively expected due to their higher stiffnesses. It is also noted that the shorter beams are associated with substantially larger regions of instability where the unstable regions for a beam of length $L = 0.8$ are almost three times that for a beam of length $L = 1.2$. In Fig. 3, the rotating speed is varied. As expected, the higher the speed, the higher along the excitation frequency axis will be the position of the unstable region. Further, the region sizes are observed to increase with decreasing speeds.

In Fig. 4, the crack depth is varied for a beam with a single crack at the mid-point. It is observed that the variation of the results is minimal if the crack is shallow, i.e. $a/h < 0.5$. However, when the crack becomes deeper, i.e. $a/h > 0.5$, there is appreciable change in the position of the unstable regions. It is observed that the increases in the crack depths shift the unstable regions to the left on the frequency axis, which can be attributed to the overall reducing stiffness due to the increasing severity of the crack. Also, it is interesting to note that the sizes of the unstable regions increase moderately with the crack severity, especially for the second mode. In Fig. 5, the position of the crack is varied. There is no clear trend that can be drawn from the results with regards to the unstable region characteristics. However, it is observed that the unstable region sizes are not sensitive to variation in the crack position. The results also show that effects of increasing crack depth are slightly more influential on the higher modes with minimal effects on the fundamental mode.

Figures 6 to 9 are the corresponding results to Figs 2 to 5 for a beam with double cracks in relatively close proximity. The cracks are a distance $0.1L$ apart from each other and their position are defined by a mean position parameter

$$\overline{x}_{cmean} = \frac{\overline{x}_{c1} + \overline{x}_{c2}}{2} \tag{31}$$

where $\overline{x}_{c1}$ and $\overline{x}_{c2}$ are the distances of the two cracks from the centre of the hub. The results for the beam with double cracks show similar trends to that of the single crack beam except that the unstable regions are generally lower on the excitation frequency axis with larger sizes attributable to the lower stiffnesses.

4. Conclusions

The dynamic stability of a rotating blade containing transverse cracks has been modeled based upon crack release energy approach in conjunction with Hamilton's principle and the assumed-mode method. Bolotin's first approximation was used to obtain the principal instability regions. Further, it was observed that there were no qualitative changes in the instability regions due to the cracks. The quantitative changes due to variations in blade length, rotational speed, crack depth and crack location have been discussed in detail.

References

[1] R.D. Adams, P. Cawley, C.J. Pye and B.J. Stone, A vibration technique for non-destructively assessing the integrity of structures, *Journal of Mechanical Engineering Science* **20** (1978), 93–100.

[2] F.D. Ju, M. Akjun, T.L. Paez and E.T. Wong, Diagnosis of fracture damage in simple structures, *Bureau of Engineering Research Report No. CE-62(82)AFOSR-993-1*, University of New Mexico, Albuquerque, NM, 1982.

[3] N. Moshrefi, H.A. Sreshta and W.T. Springer, The transverse vibration characteristics of an externally damaged pipe, in: *Vibration Analysis to Improve Reliability and Reduce Failure*, P.M. Niskode and P.E. Doepker, eds, ASME, New York, 1985, pp. 23–29.

[4] F.D. Ju and M.E. Mimovich, Experimental diagnosis of fracture damage in structures by the modal frequency method, *Journal of Vibration, Acoustics, Stress and Reliability in Design* **110** (1988), 456–463.

[5] P.F. Rizos, N. Aspragathos and A.D. Dimarogonas, Identification of crack location and magnitude in a cantilever beam from the vibration modes, *Journal of Sound and Vibration* **138** (1990), 381–388.

[6] P. Gudmundson, Eigenfrequency changes of structures due to cracks, notches or other geometrical changes, *Journal of the Mechanics and Physics of Solids* **30** (1982), 339–353.

[7] P. Gudmundson, The dynamic behavior of slender structures with cross-section cracks, *Journal of the Mechanics and Physics of Solids* **31** (1983), 228–345.

[8] C.A. Papadopoulos and A.D. Dimarogonas, Coupled longitudinal and bending vibrations of a cracked shaft, *Journal of Vibration, Acoustics, Stress and Reliability in Design* **110** (1988), 1–8.

[9] C.A. Papadopoulos and A.D. Dimarogonas, Stability of cracked rotors in coupled mode vibration, *Journal of Vibration, Acoustics, Stress and Reliability in Design* **110** (1988), 356–359.

[10] B.S. Haisty and W.T. Springer, A general beam element for use in damage assessment of complex structures, *Journal of Vibration, Acoustics, Stress and Reliability in Design* **110** (1988), 389–394.

[11] G.L. Qian, S.N. Gu and J.S. Jiang, The dynamic behavior and crack detection of a beam with a crack, *Journal of Sound and Vibration* **138** (1990), 233–243.

[12] T.G. Chondros and A.D. Dimarogonas, Dynamic sensitivity of structures to cracks, *Journal of Vibration, Acoustics, Stress and Reliability in Design* **111** (1989), 251–256.

[13] M.H.H. Shen and C. Pierre, Natural modes of Bernoulli-Euler beams with symmetric cracks, *Journal of Sound and Vibration* **138** (1990), 115–134.

[14] A.D. Dimarogonas and S.A. Paipetis, *Analytical Methods in Rotor Dynamics*, Applied Science, London, 1983.

[15] A.D. Dimarogonas and C.A. Papadopoulos, Vibration of a cracked shaft in bending, *Journal of Mechanical Design* **102** (1983), 140–146.

[16] R.L. Sutherland, Bending vibration of a rotating blade vibrating in the plane of rotation, *Journal of Applied Mechanics* **16** (1949), 389–394.

[17] M.L. Renard and J.E. Rabowski, Equatorial vibrations of a long flexible boom on a spin stabilized satellite of non-zero radius, *Proceedings of the 21st Congress of the International Astronautical Federation*, Mar Del Plata, Argentina, 1970, pp. 35–53.

[18] P.W. Likins, F.J. Barbera and V. Baddeley, Mathematical modeling of spinning elastic bodies for modal analysis, *AIAA Journal* **11** (1973), 1251–1258.

[19] G.L. Anderson, On the extensional and flexural vibrations of rotating bars, *International Journal of Non-Linear Mechanics* **10** (1975), 223–236.

[20] M. Swaminathan and J.S. Rao, Vibrations of rotating pretwisted and tapered blades, *Mechanism and Machine Theory* **12** (1977), 331–337.

[21] D.H. Hodges and J. Ruthoski, Free vibration analysis of rotating beams by variable-order finite element method, *AIAA Journal* **19** (1981), 1459–1466.

[22] K.B. Subrahnanvam, S.V. Kulkarni and J.S. Rao, Application of the Reissner method to derive the coupled bending-torsion equations of dynamic motion of rotating pretwisted cantilever blading with allowance of shear deflection, rotary inertia, warping and thermal effects, *Journal of Sound and Vibration* **84** (1982), 223–240.

[23] T.R. Kane, R.R. Ryan and A.K. Banerjee, Dynamics of a cantilever beam attached to a moving base, *Journal of Guidance, Control and Dynamics* **10** (1987), 139–151.

[24] C.E. Hammond, An application of Floquet theory to prediction of mechanical instability, *Journal of the American Helicopter Society* **19** (1974), 14–23.

[25] V.V. Bolotin, *The Dynamic Stability of Elastic Systems*, Holden-Day, San Francisco, 1983.

[26] M.C. Wu and S.C. Huang, On the vibration of a cracked rotating blade, *Shock and Vibration* **5** (1998), 317–323.